Current Applied Physics 17 (2017) 584–591

Contents lists available at ScienceDirect

Current Applied Physics

journal homepage: www.elsevier.com/locate/cap

Adjust band gap of IATO nanoparticles to obtain desirable optical property by one-step hydrothermal oxidation

Te Hu [a, b, c], Yuchang Su [a, *], Ian R. Baxendale [b], Jiang Tan [a], Hongbo Tang [a], Lihua Xiao [a], Feng Zheng [a], Ping Ning [d]

[a] School of Materials Science and Engineering, Central South University, South Lushan Road, Changsha 410083, China
[b] Department of Chemistry, Durham University, South Road, Durham DH1 3LE, United Kingdom
[c] Faculty of Science, Kunming University of Science and Technology, South Jingming Road, Kunming 650500, China
[d] Faculty of Environment Science and Engineering, Kunming University of Science and Technology, South Jingming Road, Kunming 650500, China

ARTICLE INFO

Article history:
Received 11 July 2016
Received in revised form
19 October 2016
Accepted 16 January 2017
Available online 19 January 2017

Keywords:
Hydrothermal oxidation
Metal oxide
Optical property
Band gap energy
Nanoparticles
IATO
Synthesize

ABSTRACT

Antimony-tin-doped indium oxide (IATO) as transparent conducting oxide (TCO) exhibits significant optical property on blocking UV and Infrared(IR) for wavelengths less ~400 nm and over ~1400 nm as well as appropriate transmissivity on visible wavelength in our work that can be as an optional idea optical material applying in shielding film or nanocomposite to achieve desired optical application.

We have successfully developed an optimal synthesis system which allows for a single hydrothermal oxidation directly synthesizing IATO nanoparticles without high-temperature calcination. These nanoparticles show superior size, crystallinity, agglomeration and are free of intermediates $In(OH)_3$ and InOOH. We also have demonstrated they give scope to desired optical property as a result of an altered IATO band gap energy.

We highlight this approach due to the shortened preparation time, the reduced energy consumption and the decreased chemical usage which dramatically save on production costs and protect environment.

1. Introduction

Transparent conducting oxides (TCO) are particularly attractive on optical application including functional glass [1,2], solar cells [3,4], smart windows [5,6] and electrode [7,8] over the last decade.

ITO [9–19] and ATO [20–30] as classic members of TCO have been extensively reported in recent years. These metal oxides are generated by diverse synthesis methods including hydrothermal [20,29], sintering [10,13], sol-gel [15,16,24,28], hydrothermal followed sintering [15,26] or sol-gel followed sintering [9,11,12,14,20,24] with certain doping ratio and materials under distinct reaction time and treatment temperature making synthesized nanomaterials exhibit specific crystalline structure [9,12,13,15,23,26,28], agglomeration level [12,13,15,21] and particle size [12–15,21,23,28] that result in band gap [11,12,15,16,20,26] of product is altered then performing certain optical property. However, their instinctive screening UV or IR wavelength is inefficiency [9,16,25,28] that can be optimized by changing thickness [10–12,17,18,23,27,28], layers [9,25,28], concentration [16,22,23,28–30] and materials of coating [25] or compositing with specific polymers [11,20] but that make their optical applications complicated and some results are still in unsatisfactory [10,17–19,22,27,29,30].

Meanwhile, over 24 h reaction time [9,11,15,23,27], high energy consumption on calcination procedure for nanoparticles crystallization [9,11,16,23], additional capping and anion-exchange agents usage [15,16] and preparation under N2, H2, Ar atmosphere [11,15,19,27] make synthesis of nanomaterials complicated and high cost.

On account of these reasons it would be highly desirable to synthesize a particular TCO material with efficient blocking on UV and IR wavelength and simple synthetic procedure to enhance potential in optical application. Therefore, we have successfully established one-step synthetic system to prepare IATO by hydrothermal oxidation [31–37] and achieved decreasing particle size and aggregation level and eliminating impurities $In(OH)_3$ and InOOH [38–43] due to their undesirable optical property [42,43] to optimize band gap for IATO possessing notable optical property on blocking UV and IR as well as suitable visible region transparency.

* Corresponding author.
E-mail address: ychsu@csu.edu.cn (Y. Su).

http://dx.doi.org/10.1016/j.cap.2017.01.011
1567-1739/

2. Experimental

We started our investigation by evaluating the various reaction parameters through an iterative combinatorial approach. The Indium was first dissolved in hydrochloric acid formed Indium salt ($InCl_3$) then mixed with tin(IV) chloride pentahydrate ($SnCl_4 \cdot 5H_2O$), antimony chloride ($SbCl_3$) and urea in a mixed solvent system containing different proportions of deionized water, EG (ethylene glycol) and 1-butanol. A standard reaction molar ratio of inorganics was maintained during the investigation: $[In_3^+]/[Sn_4^+] = 20/1$, $[In_3^+]/[Sb_3^+] = 19/1$, and $[In_3^+]/[OH^-] = 1/3$.

The resulting suspension was diffused by magnetic stirring for 1 h at ambient temperature and then poured into a Teflon-lined reactor and heated at different reaction temperatures (160 °C, 180 °C and 200 °C) for various reaction times (6 h, 12 h, 18 h, 24 h, 48 h and 72 h). After cooling, the obtaining colloidal products were collected as blue-gray solids by centrifugal separation and subsequently the solids were purified in deionized water by ultrasonic dispersion and magnetic stirring. Sequence of collection and depuration was repeated until the washings gave a positive indication for chloride ions. The products were dried in a microwave oven (80% power at 850 W) for 15 min and then manually ground to a fine powder using an agate mortar.

Crystalline phases of all IATO products were recorded using X-ray diffraction (XRD) on a Rigaku D/Max 2500 measurement system (Japan). Sizes and morphologies of IATO nanoparticles were measured by transmission electron microscopy (TEM) with TecnaiG220AEM from FEI of the USA. Optical properties of the IATO nanoparticles were measured on a Lambda 750 from Perkin Elmer (USA).

3. Results and discuss

Under distinct synthetic systems IATO nanoparticles has various band gaps giving play to unique optical properties. A series of systematic experiment and analysis has been completed to select the optimized combination of reactant, solvent composition, hydrothermal temperature and reaction time for IATO nanoparticles obtaining desirable optical property.

3.1. Effect of content of deionized water and hydrothermal oxidation temperature on formation of IATO nanoparticles

Water is strong polar solvent capable of solubilizing $InCl_3$, $SnCl_4$ and $SbCl_3$ and known to hydrolyze urea to ammonia thereby generating nucleophilic hydroxide ions for the preparation of $In(OH)_3$. The $In(OH)_3$ initially formed is partly converted into InOOH through dehydration with increasing temperature. Ultimately, control experiments have proved proportion of deionized water in solvent system and hydrothermal temperature are key factors on IATO hydrothermal reaction. Fig. 1 shows the XRD crystalline phases of the different products synthesized using diverse proportions

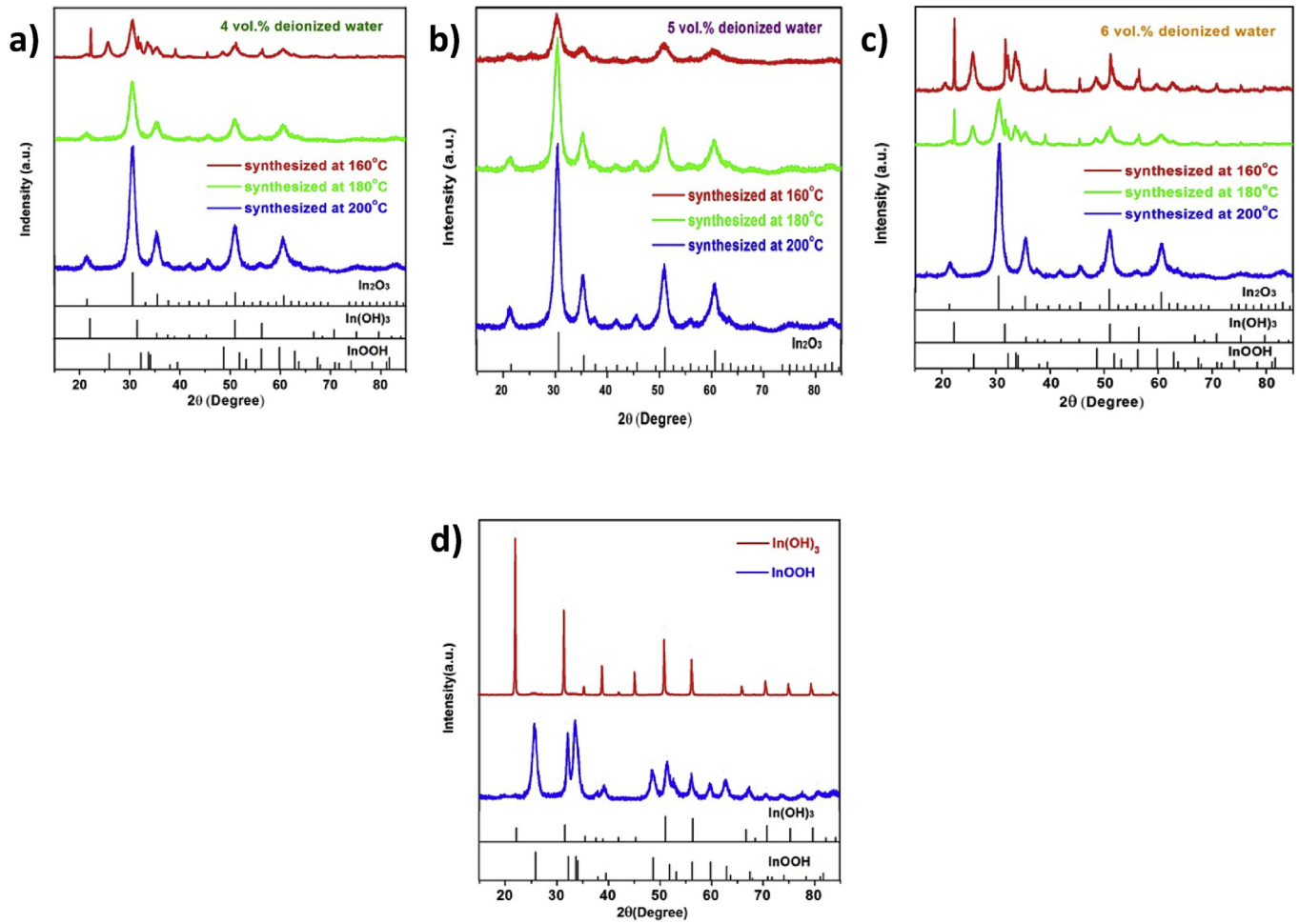

Fig. 1. Crystalline phases of IATO nanoparticles synthesized with various contents of deionized water at different temperatures for 24 h a), b) and c) Using 4 vol%, 5 vol% and 6 vol% deionized water respectively to synthesize products at different hydrothermal temperatures (160 °C, 180 °C, 200 °C) for 24 h. d) XRD patterns of $In(OH)_3$ and InOOH.

of deionized water (4 vol%, 5 vol% and 6 vol%) at different hydrothermal temperatures (160 °C, 180 °C and 200 °C) for 24 h.

It can be seen that when using 6 vol% deionized water and preparing at a temperature of 160 °C the products are mixture of cubic $In(OH)_3$ and orthorhombic InOOH. Synthesized mixture contains a certain amount of cubic In_2O_3 except for cubic $In(OH)_3$ and orthorhombic InOOH at 180 °C and the two intermediates are fully converted to cubic In_2O_3 at 200 °C (Fig. 1c). By contrasts when 4 vol% deionized water is employed cubic $In(OH)_3$, orthorhombic InOOH and cubic In_2O_3 present in the mixture at 160 °C but only cubic In_2O_3 is detected at the higher temperatures of 180 °C and 200 °C (Fig. 1a). Interestingly, at 5 vol% water content only cubic In_2O_3 is found in the product starting from at 160 °C, moreover, the crystallization of cubic In_2O_3 is sharper at higher hydrothermal temperatures of 180 °C and 200 °C (Fig. 1b)). It indicates that cubic In_2O_3 is more efficiently formed with 5 vol% deionized water. XRD patterns of InOOH and $In(OH)_3$ as reference is used to identify compositions of mixture as shown in Fig. 1d).

To improve the transformation efficiency of cubic $In(OH)_3$ and orthorhombic InOOH as far as possible for obtain desired cubic In_2O_3 with superior crystallization we selected the use of 5 vol% deionized water and a hydrothermal temperature of 200 °C as the basic optimal conditions for further research.

3.2. Correlation of band gap energy and optical property of IATO nanoparticles

As the optical characteristics of TCO nanomaterials are closely relate to the band gap energy [27–34], therefore, altering the band gap energy of IATO nanoparticles is an efficient and direct method to change the transmittance of the IATO nanoparticles.

3.2.1. Investigating the impact of hydrothermal reaction time on the band gap energy of the IATO nanoparticles

According to comparative experiments, they were shown that hydrothermal reaction time can change the aggregation level, size and purity of IATO nanoparticles to regulate the band gap energy of IATO nanoparticles.

Fig. 2 illustrates the XRD crystalline phases of the different products synthesized at 200 °C for a range of reaction times (6 h, 18 h, 24 h, 48 h and 72 h) using 95 vol% EG (ethylene glycol) and 5 vol% deionized water. Analysis of the reactions on 6 h and 18 h indicates that the cubic $In(OH)_3$ and orthorhombic InOOH are partially converted into cubic In_2O_3. Further prolonging the reaction time to 24 h, 48 h and 72 h the cubic $In(OH)_3$ and orthorhombic InOOH are completely transformed into the cubic In_2O_3.

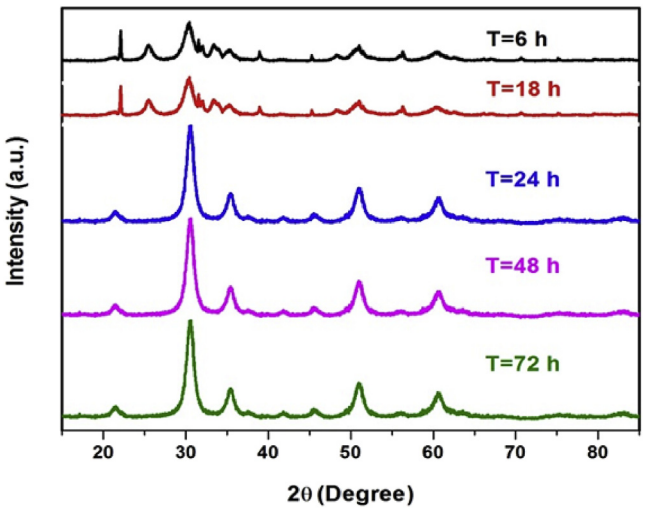

Fig. 2. Crystalline phases of IATO nanoparticles synthesized at 200 °C for different hydrothermal reaction times. (T presents reaction time).

Fig. 3 shows TEM images of IATO nanoparticles prepared at hydrothermal temperature of 200 °C using 95 vol% EG (ethylene glycol) and 5 vol% deionized water but for various reaction times that presents size and agglomeration of the nanoparticles are positively related to reaction time.

Fig. 4a displays change of band gap energy E_g of synthesized IATO nanoparticles with diverse hydrothermal reaction times and corresponding transmittance data as shown in Fig. 4b was measured by UV–Vis–NIR Spectrophotometer and used for determine an E_g value. The band gap energy E_g is estimated using extrapolation equation $\alpha h\nu = A(h\nu - E_g)^n$ to plot a graph of $(\alpha h\nu)^{1/n}$ and $h\nu$, in the equation, α is the absorption coefficient, h is Planck constant, $h\nu$ is the incident photon energy, A is a constant and exponent n values 1/2, 2, 3/2 and 3 relating to allowed direct, allowed indirect, forbidden direct and forbidden indirect transitions, respectively. For cubic IATO nanocrystals, the value of exponent n is taken as 1/2 for direct transition to obtain band gap energy E_g by employing intercept method on the curve graph of $(\alpha h\nu)^2$ and $h\nu$. Depending on this way, the lowest band gap energy of 2.54 eV is obtained as shown in Fig. 5 the corresponding nanoparticles synthesized at 200 °C for 24 h in Fig. 4a and its relevant optical property is more particular according to Fig. 4b.

Expect for analyzing change of optical property of nanomaterials with band gap energy, we can use localized surface plasmon resonance (LSPR) to explain distinction of the optical property because it is associates with nanostructures to create specific spectral absorption due to molecular interactions near the nanoparticle surface. A plasmon is a collective oscillation of the free electrons in nanoparticle.

In detail some of the many factors that can affect LSPR sensitivity, including nanoparticle size, shape, and material composition [44].

According to characterization from XRD (Fig. 2) and TEM (Fig. 3), at 200 °C for 24 h synthesized IATO nanoparticles with distinctive size, shape and composition comparing with other IATO nanoparticles under various preparing conditions make its localized surface plasmon resonance differ with other products thus displays unique optical property.

We therefore selected 24 h as the preferred hydrothermal reaction time for preparation of IATO nanoparticles in the following experiments.

To explain the relationship between the band gap energy of the products and optical properties we initially make the assumption that the synthesized individual IATO nanoparticle is sphere.

Intrinsic gap band of TCO nanomaterials decides particular wavelength absorption property [9,11,26] thereby shift of the band gap depending on changes in size, agglomeration level and purity of IATO nanoparticles resulting in diverse optical characteristics has been demonstrated in Fig. 6. Refer to Figs. 2 and 3 the hydrothermal reaction time is prolonged to 48 h and 72 h the cubic $In(OH)_3$ and orthorhombic InOOH components are completely converted into cubic In_2O_3 but the size of IATO nanoparticles is increased. In this situation, light cannot penetrate the entire IATO nanoparticle with only the exterior part of nanoparticles capable of absorbing the incident light. Therefore for amount of interior of nanoparticles is incapable of interacting with the light which results in a change of the band energy gap and the products display a corresponding transmittance. By comparison for these shorter reaction times 6 h and 18 h the size of nanoparticles is dwindled then light can pass through the entire nanoparticles, however, the presence of cubic $In(OH)_3$ and orthorhombic InOOH leads to these samples obtain

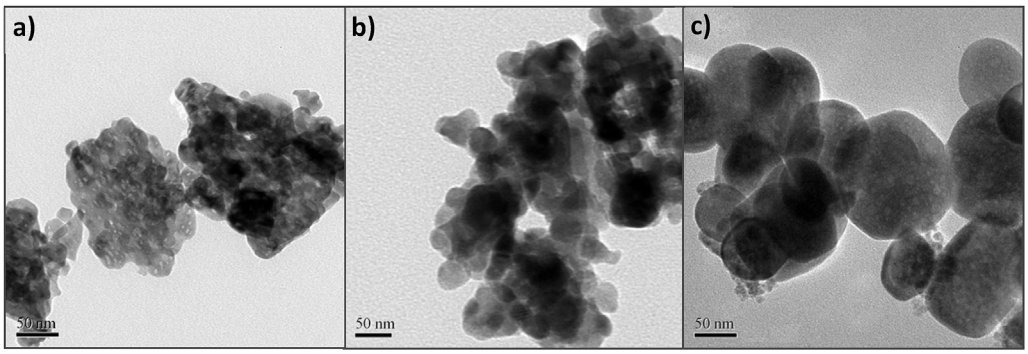

Fig. 3. TEM images of IATO nanoparticles under at 200 °C employing 95 vol% EG (ethylene glycol) and 5 vol% deionized water for diverse reaction times: a) 6 h, b) 24 h and c) 72 h.

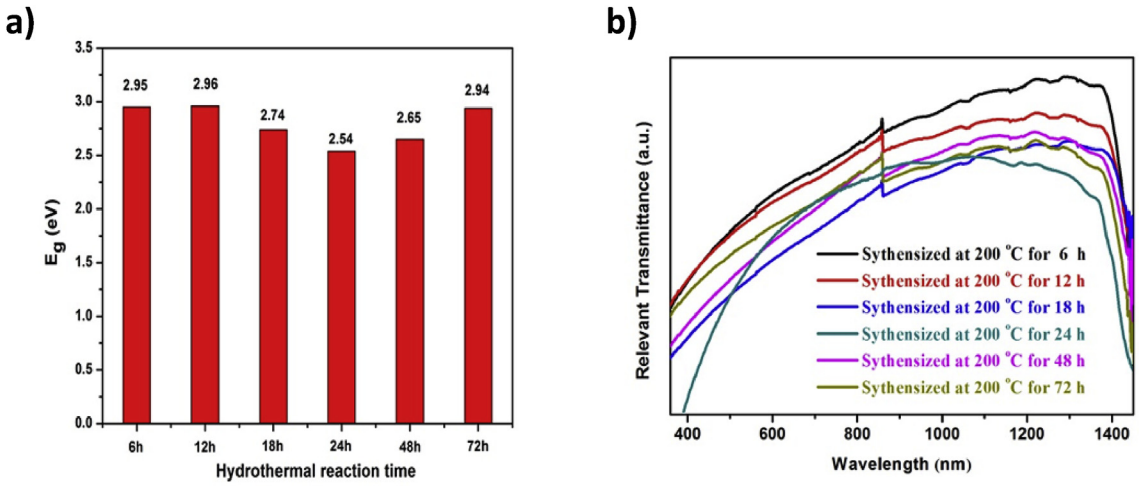

Fig. 4. a) Band gap energies of IATO nanoparticles synthesized at 200 °C for different hydrothermal reaction times. b) Transmittance of IATO nanoparticles synthesized at 200 °C for different hydrothermal reaction times.

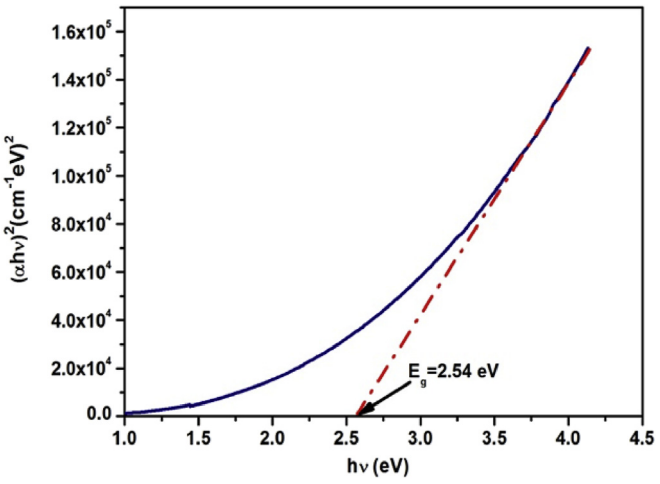

Fig. 5. Band gap energy of IATO nanoparticles synthesized at 200 °C for 24 h.

undesired transmittance.

Interestingly, using 24 h as the reaction time not only IATO nanoparticles are pure cubic In_2O_3 without cubic $In(OH)_3$ and orthorhombic InOOH but also appropriate size of the nanoparticles allows light almost entirely pass through the whole nanoparticles resulting in distinguishing transmittance due to the lowest band gap energy as shown in Fig. 5. For these reasons 24 h was selected as optimum as the hydrothermal reaction time.

However, sufficient chlorine ions remain in this reaction system causing severe agglomeration of nanoparticles [21] regardless of how long reaction time is and diverse purity and size of IATO nanoparticles result in obtained band gap energy of IATO nanoparticle can not reveal satisfactory optical property thus further optimizing purity and size of IATO nanoparticles and restraining aggregation of nanoparticles are crucial factor s to obtain appropriate band gap energy for gain desirable optical property.

3.2.2. The effect proportion of 1-butanol on the band gap energy of IATO nanoparticles

The use of 1-butanol as a dispersant is beneficial due to its weak polarity [45–47] and low chemical coordinating ability [48–49] thus which can retard aggregation of IATO nanoparticles and improve the size and purity of IATO nanoparticle to change the band gap energy for gain the desired optical properties.

Fig. 7 displays the XRD crystalline phases of the different products synthesized at 200 °C for 24 h with different proportions of 1-butanol (0 vol%, 5 vol%, 10 vol%, 15 vol%, 18 vol%, 20 vol%, 40 vol % and 60 vol%) and a corresponding volume of EG and 5 vol% deionized water.

The results indicate the products generally contain cubic $In(OH)_3$, orthorhombic InOOH and cubic In_2O_3 when the higher amounts of 1-butanol are used (40 vol% and 60 vol%). In contrast the products contain only cubic In_2O_3 when lower proportions of 1-butanol are employed (0, 5 vol%, 10 vol%, 15 vol%, 18 vol% and 20 vol%).

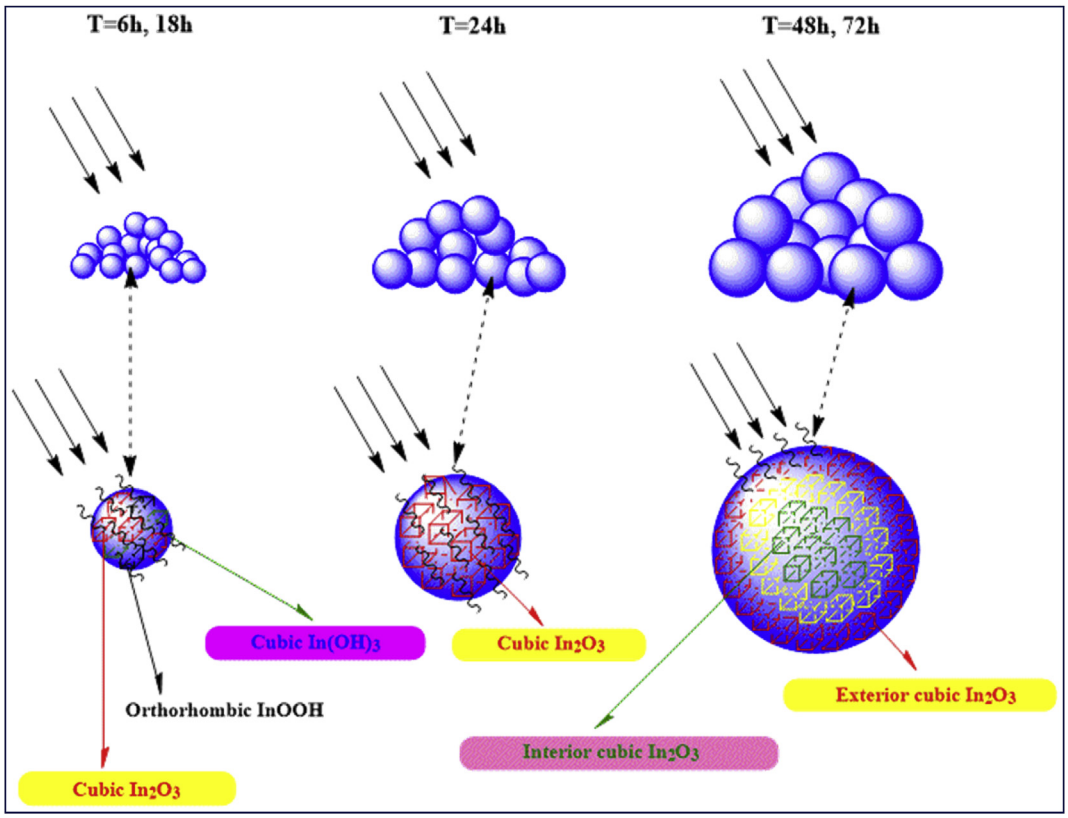

Fig. 6. Different reaction time affects size, purity and aggregation of nanoparticles. (T presents reaction time).

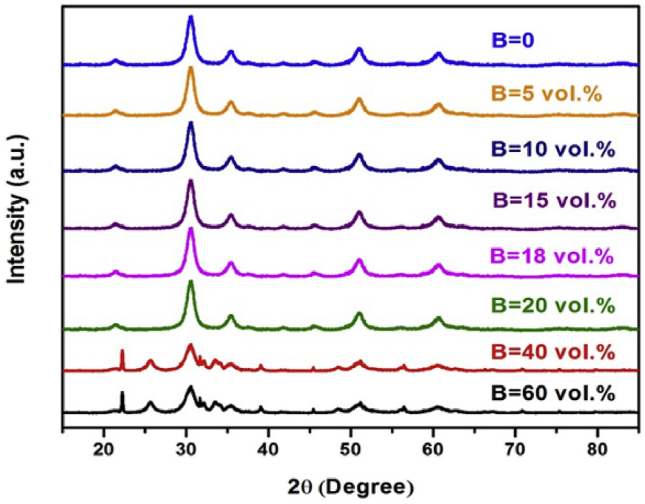

Fig. 7. Crystalline phases of IATO nanoparticles synthesized at 200 °C for 24 h with diverse proportions of 1-Butanol. (B presents certain proportion of 1-butanal in mixed solvent system).

Fig. 8 presents TEM images of IATO nanoparticles synthesized at 200 °C for 24 h with diverse proportions of 1-Butanol that proves size of the nanoparticles has been significantly decreased comparing with Fig. 3 without 1-Butanol and agglomeration is observably improved by adding content of 1-Butanol.

Fig. 9a shows the band gap energy of IATO nanoparticles is altered when IATO nanoparticles are synthesized in mixed solvent systems comprising of different proportions of 1-butanol and matched transmittance of IATO nanoparticles as shown in Fig. 9b. The lowest band gap energy of 1.93 eV is achieved for 20 vol% 1-butanol and corresponding satisfactory transmittance displays prominently blocking UV and Infrared(IR) for wavelengths less ~400 nm and over ~1400 nm as well as appropriate transparency on visible wavelength as shown in Fig. 9c and d individually.

Fig. 10 illustrates purity, agglomeration and size of nanoparticle are changed by varying the amount of 1-butanal as a dispersant.

Although size and purity of nanoparticles are availably promoted when choosing lower proportions of 1-butanol (0, 5 vol%, 10 vol%, 15 vol% and 18 vol%), aggregation level of IATO nanoparticles is not up to suitable condition in consequence leading to gain undesired transmittance from corresponding band gap energy.

By comparison when the higher proportions of 1-butanol (40 vol% and 60 vol%) were used the size and agglomeration of product are markedly improved but the presence of cubic $In(OH)_3$ and orthorhombic InOOH unsatisfactory transmittance is obtained from relevant band gap energy.

The most satisfactory transmittance in our work was acquired from samples prepared using 20 vol% of 1-butanol. These nanoparticles just contain cubic In_2O_3 without cubic $In(OH)_3$ and orthorhombic InOOH and have appropriate size and aggregation degree leading to a featured energy band gap making IATO nanoparticles obtain desired optical property as obviously cut off wavelength for less ~400 nm and over ~1400 nm as well as apt visible light transparent.

Based on an overview of our current results it can be concluded that in order to tune the band gap energy of the IATO nanoparticles to obtain satisfactory optical characteristic so the optimal reaction parameters have to be chosen by comparative experiments to improve size, purity and agglomeration of the IATO nanoparticles.

Fig. 11 displays size and crystallization of IATO nanoparticles which were synthesized by hydrothermal oxidation reaction in a

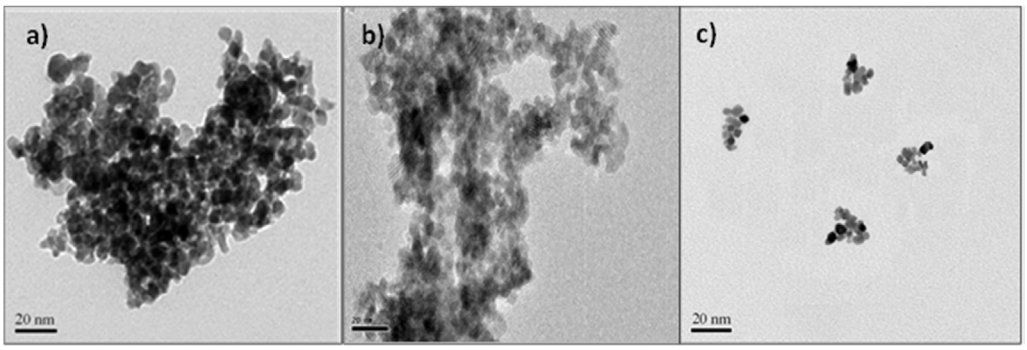

Fig. 8. TEM images of IATO nanoparticles synthesized at 200 °C for 24 h with different proportions of 1-Butanol in solvent system: a) 10 vol%, b) 20 vol% and c) 60 vol%.

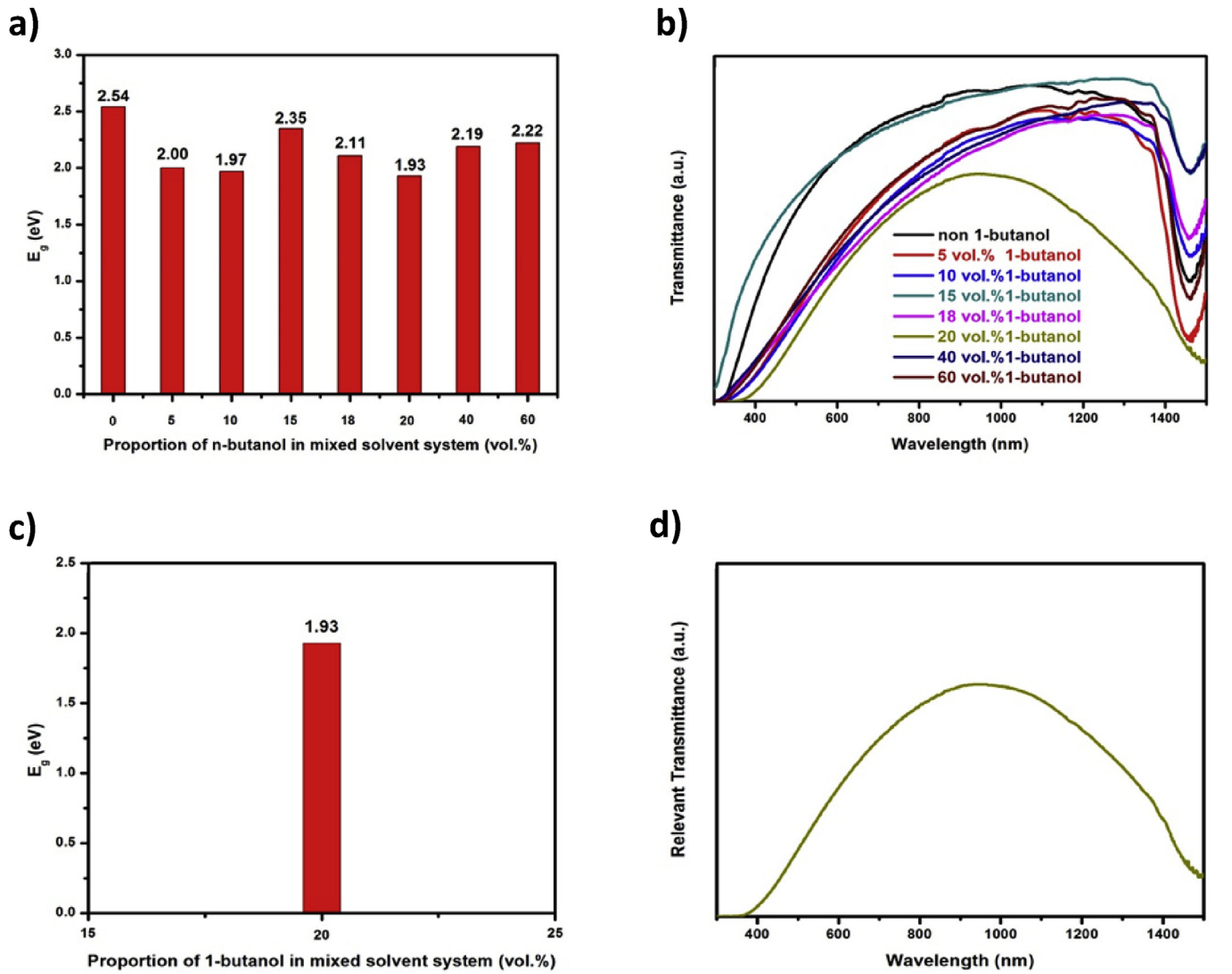

Fig. 9. a) Band gap energies of IATO nanoparticles synthesized with different proportions of 1-butanal in mixed solvent system at 200 °C for 24 h. b) Transmittance of IATO nanoparticles synthesized with different proportions of 1-butanal in mixed solvent system at 200 °C for 24 h. C) Band gap energy of IATO nanoparticles synthesized with 20 vol% of 1-butanal in mixed solvent system at 200 °C for 24 h. d) Transmittance of IATO nanoparticles synthesized with 20 vol% of 1-butanal in mixed solvent system at 200 °C for 24 h.

mixed solvent with 5 vol% deionized water, 20 vol% 1-butanol and 75 vol% EG at 200 °C for 24 h.

The IATO nanoparticles formed under these optimized conditions are on average ~10 nm with good dispersion and low agglomeration in Fig. 11a. A selected mini zone with red box as shown in the upper right of Fig. 11b is amplified in Fig. 11c that highlighting the interplanar spacing which is measured as 0.927 nm. Fig. 11d shows a (222) lattice plane of cubic In_2O_3 according to Fast Fourier Transfer (FFT) analysis of the selected zone with red box.

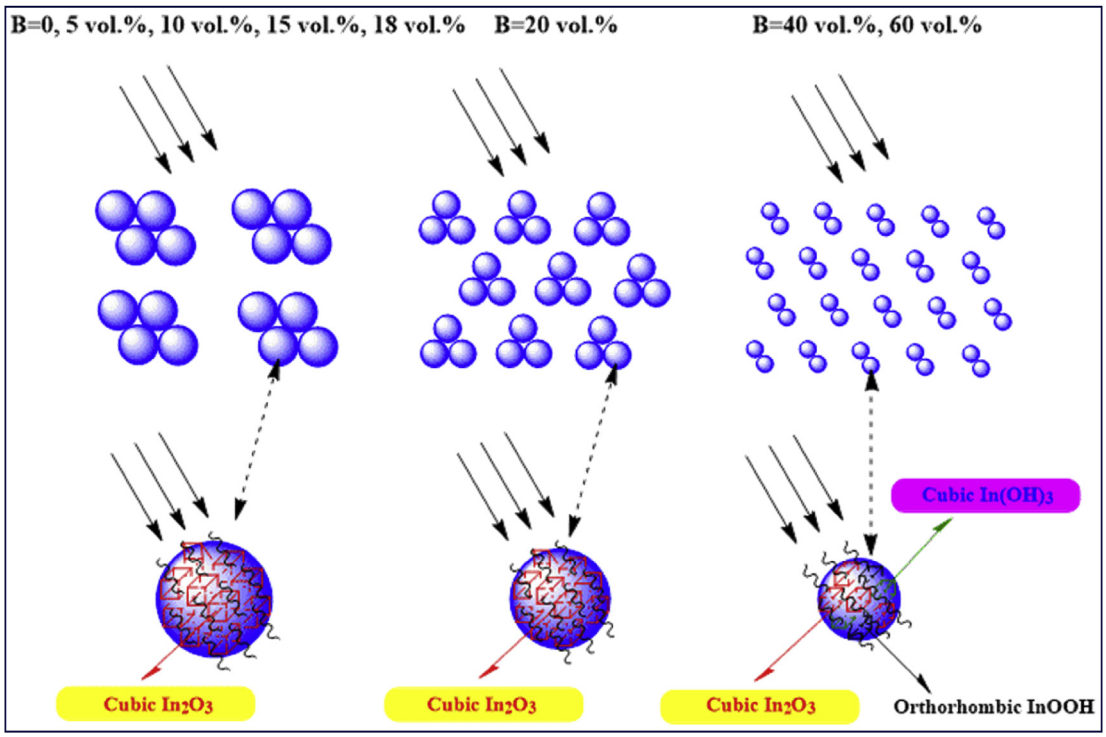

Fig. 10. Different proportions of 1-butanal affect upon size, purity and aggregation of nanoparticles. (B presents certain proportion of 1-butanal in solvent system).

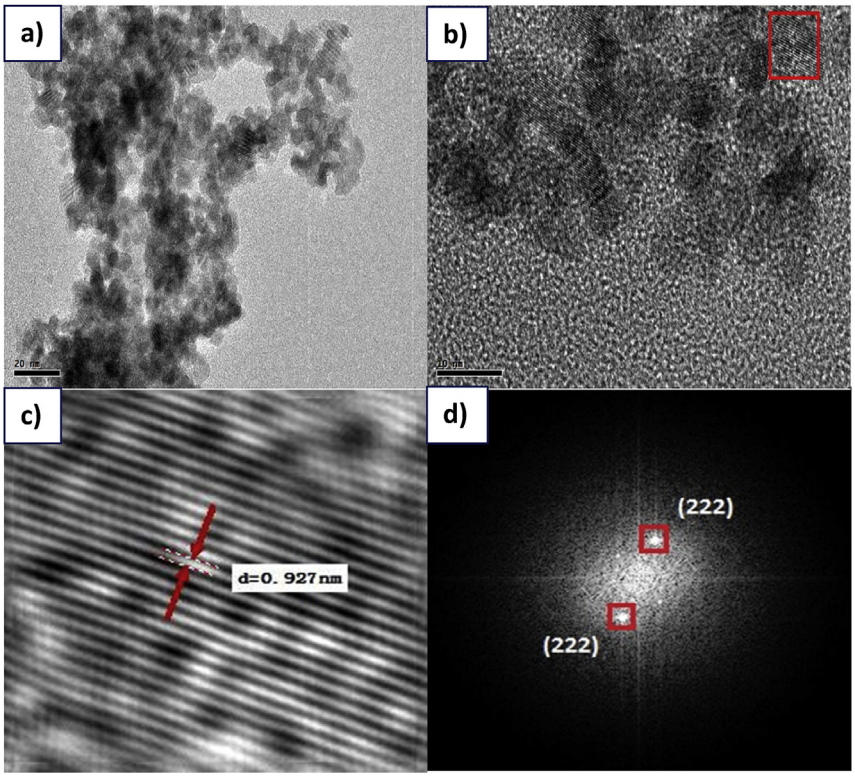

Fig. 11. a) TEM image of IATO nanoparticles; b) HRTEM image of IATO nanoparticles; c) Amplification on selected red zone in the HRTEM image of IATO nanoparticles; d) FFT image of IATO nanoparticles on selected red zone. (For interpretation of the references to colour in this figure legend, the reader is referred to the web version of this article.)

4. Conclusion

We have successfully shown that the optical property of IATO nanoparticles can be altered from change of corresponding band gap energy of IATO nanoparticles using a one-step hydrothermal oxidation. Ultimately, we acquired optimized experimental

parameters through a series of contrast experiments: a prime mixed solvent system was comprised of 5 vol% deionized water, 20 vol% 1-bunatol and 75 vol% EG and a best suitable hydrothermal oxidation condition was at 200 °C for 24 h. These conditions make IATO nanoparticles which possess superior purity, size, crystallinity and agglomeration and obtain satisfactory optical property from specific band gap energy that could efficiently block UV and IR for wavelengths less ~400 nm and over ~1400 nm and allow visible wavelength with appropriate transmittances for more potential optical application.

In the simplified experimental procedure the need for calcination is removed and intermediates $In(OH)_3$ and InOOH are availably transformed into In_2O_3. In addition, efficiently reducing energy consumption, shorting experimental cycle time and decreasing chemical usage can be achieved in the preparation processes.

References

[1] B.G. Lewis, D.C. Paine, MRS Bull. 25 (2000) 22.
[2] J. Lacombe, O. Sergeev, K. Chakanga, K.V. Maydell, C. Agert, J. Appl. Phys. 110 (2011) 023102.
[3] O.K. Varghese, M. Paulose, C.A. Grimes, Nat. Nanotechnol. 4 (2009) 592.
[4] N. Kim, H. Um, I. Choi, K. Kim, K. Seo, ACS Appl. Mater. Interfaces 8 (2016) 11412.
[5] C.G. Granqvist, Sol. Energy Mat. Sol. Cells 91 (2007) 1529.
[6] J. Montero, C. Guillén, C.G. Granqvist, J. Herrero, G.A. Niklasson, J. Appl. Phys. 115 (2014) 153702.
[7] J.Z. Song, H.B. Zeng, Angew. Chem. Int. Ed. 54 (2015) 9760.
[8] J.Z. Song, S.A. Kulinich, J.H. Li, Y.L. Liu, H.B. Zeng, Angew. Chem. Int. Ed. 54 (2015) 462.
[9] C. Goebbert, R. Nonninger, M.A. Aegerter, H. Schmidt, Thin Solid Films 351 (1999) 79.
[10] H. Kim, C.M. Gilmore, A. Piqué, J.S. Horwitz, H. Mattoussi, H. Murata, Z.H. Kafafi, D.B. Chrisey, J. Appl. Phys. 86 (1999) 6451.
[11] M.A. Aegerter, N. Al-Dahoudi, J. Sol-Gel Sci. Technol. 27 (2003) 81.
[12] J. Ederth, P. Heszler, A. Hultåker, G.A. Niklasson, C.G. Granqvist, Thin Solid Films 445 (2003) 199.
[13] A. Solieman, M.A. Aegerter, Thin Solid Films 502 (2006) 205.
[14] Z.H. Li, Y.P. Ke, D.Y. Ren, Trans. Nonferrous Met. Soc. China 18 (2008) 366.
[15] P. Tao, A. Viswanath, L.S. Schadler, B.C. Benicewicz, R.W. Siegel, ACS Appl. Mater. Interfaces 3 (2011) 3638.
[16] H.R. Xu, H.Y. Zhou, G.S. Zhu, J.Z. Chen, C.T. Liao, Mater. Lett. 60 (2006) 983.
[17] M.M. El-Nahass, E.M. El-Menyawy, Mater. Sci. Eng. B Adv. 177 (2012) 145.
[18] A. Eshaghi, A. Graeli, Optik 125 (2014) 1478.
[19] J.H. Lee, S.H. Lee, G.L. Li, M.A. Petruska, D.C. Paine, S.H. Sun, J. Am. Chem. Soc. 134 (2012) 13410.
[20] J.P. Coleman, A.T. Lynch, P. Madhukar, J.H. Wagenknecht, Sol. Energy Mat. Sol. Cells 56 (1999) 375.
[21] J.R. Zhang, L. Gao, Mater. Chem. Phys. 87 (2004) 10.
[22] G. Jain, R. Kumar, Opt. Mater. 26 (2004) 27.
[23] H.J. Jeon, M.K. Jeon, M. Kang, S.G. Lee, Y.L. Lee, Y.K. Hong, B.H. Choi, Mater. Lett. 59 (2005) 1801.
[24] G. Guzman, B. Dahmani, J. Puetz, M.A. Aegerter, Thin Solid Films 502 (2006) 281.
[25] B.J. Yoo, K.K. Kim, S.H. Lee, W.M. Kim, N.G. Park, Sol. Energy Mat. Sol. 92 (2008) 873.
[26] A. Klein, C. Körber, A. Wachau, F. Säuberlich, Y. Gassenbauer, S.P. Harvey, D.E. Proffit, T.O. Mason, Materials 3 (2010) 4892.
[27] T.M. Hammad, N.K. Hejazy, Int. Nano Lett. 1 (2011) 123.
[28] L. Luo, D. Bozyigit, V. Wood, M. Niederberger, Chem. Mater. 25 (2013) 4901.
[29] J.M. Xu, L. Li, S. Wang, H.L. Ding, Y.X. Zhang, G.H. Li, CrystEngComm 15 (2013) 3296.
[30] S. Gürakar, T. Serin, N. Serin, Appl. Surf. Sci. 352 (2015) 16.
[31] S. Sōmiya, R. Roy, Bull. Mater. Sci. 23 (2000) 453.
[32] P. Dutournié, J. Mercadier, C. Aymonier, A. Gratias, F. Cansell, Ind. Eng. Chem. Res. 40 (2001) 114.
[33] D. Mateos, J.R. Portela, J. Mercadier, F. Marias, C. Marraud, F. Cansell, J. Supercrit. Fluid. 34 (2005) 63.
[34] K. Byrappa, T. Adschiri, Prog. Cryst. Growth Charact. Mater. 53 (2007) 117.
[35] F. Marias, F. Mancini, F. Cansell, J. Mercadier, J. Supercrit. Fluids 41 (2007) 352.
[36] A.S. Teja, P.Y. Koh, Prog. Cryst. Growth Charact. Mater. 55 (2009) 22.
[37] R.A. Kumar, M. Arivanandhan, Y. Hayakawa, Prog. Cryst. Growth Ch. 59 (2013) 113.
[38] M. Klaumünzer, M. Maćković, P. Ferstl, M. Voigt, E. Spiecker, B. Meyer, W. Peukert, J. Phys. Chem. C 116 (2012) 24529.
[39] H.H. Jiang, L.C. Zhao, L.G. Gai, L. Ma, Y. Ma, M. Li, CrystEngComm 15 (2013) 7003.
[40] M. Muruganandham, G.J. Lee, J.J. Wu, I. Levchuk, M. Sillanpaa, Mater. Lett. 98 (2013) 86.
[41] H. Zhao, W.Y. Yin, M.Y. Zhao, Y.Z. Song, H.Q. Yang, Appl. Catal. B 130–131 (2013) 178.
[42] S.Y. Chen, M.C. Wu, C.S. Lee, M.C. Lin, J. Mater. Sci. 44 (2009) 794.
[43] H.L. Zhu, K.H. Yao, H. Zhang, D.R. Yang, J. Phys. Chem. B 109 (2005) 20676.
[44] K.M. Mayer, J.H. Hafner, Chem. Rev. 111 (2011) 3828.
[45] R.Y. Hong, T.T. Pan, J.Z. Qian, H.Z. Li, Chem. Eng. J. 119 (2006) 71.
[46] J.C. Liu, J.H. Jean, J. Am. Ceram. Soc. 89 (2006) 882.
[47] A.M.L. Jackelen, M. Jungbauer, G.N. Glavee, Langmuir 15 (1999) 2322.
[48] C.J. Carrano, K.N. Raymond, J. Am. Chem. Soc. 100 (1978) 5371.
[49] K.S. Vahvaselkä, R. Serimaa, M. Torkkeli, J. Appl. Cryst. 28 (1995) 189.